

## Table of contents

|   |     |
|---|-----|
| 1. General.....   | S2  |
| 2. Preparation of dibenzofuran-based bis(1-pyrenylmethyl)diamine <b>1</b> ..... | S3  |
| 3. Preparation of two-component dyes.....                                       | S5  |
| 4. Repeated MCL of <b>1</b> and two-component dyes.....                         | S6  |
| 5. Solid-state emission properties of organic dyes.....                         | S7  |
| 6. Applicability of other preparation methods.....                              | S9  |
| 7. Mechanochromic luminescence (MCL) of two-component dyes.....                 | S10 |
| 8. Single-particle-level observations by fluorescence microscopy.....           | S14 |
| 9. Measurement of the intensity of mechanical stimuli.....                      | S17 |
| 10. Absorption properties.....  | S18 |
| 11. Proposed mechanism of the bicolor MCL.....                                  | S19 |
| 12. Solution-state studies.....   | S20 |
| 13. NMR spectra of new compounds.....   | S23 |

## 1. General

All air-sensitive experiments were carried out under an argon atmosphere unless otherwise noted. Silica gel 60 N (spherical, neutral, 63–210  $\mu\text{m}$ ) was used for column chromatography. Dibenzo[*b,d*]furan-4,6-diylidimethanol (**2**) was synthesized by a reported procedure.<sup>[1]</sup> Other reagents and solvents were commercially available and were used as received. IR spectra were recorded on a Nicolet iS10 FT-IR spectrometer.  $^1\text{H}$  and  $^{13}\text{C}$  NMR spectra were recorded on a JEOL ECA500 spectrometer or a Bruker DRX500 spectrometer using tetramethylsilane ( $^1\text{H}$  NMR: 0.00 ppm) or solvent residual signals [ $^1\text{H}$  NMR: DMSO (2.50 ppm);  $^{13}\text{C}$  NMR:  $\text{CDCl}_3$  (77.0 ppm), DMSO-*d*<sub>6</sub> (39.5 ppm)] as an internal standard. High-resolution mass spectra (HRMS) were recorded on a Hitachi Nano Frontier LD spectrometer (ESI) and a JEOL JMS-700 mass spectrometer (FAB). A miniature fiber-optic spectrometer (FLAME-S-XR1-ES, Ocean Optics) and a handy UV lamp (365 nm, LUV-6, AS ONE) were used for the measurements of mechanochromic luminescence (MCL). Fluorescence spectra were measured on a JASCO FP-8300 fluorescence spectrometer. The solid-state absorption spectra were obtained by measuring diffuse reflectance spectra using an FPA-810 powder sample cell block. The absolute fluorescence quantum yields were determined using a 100 mm  $\phi$  integrating sphere JASCO ILF-835. Powder X-ray diffraction (PXRD) measurements were performed on a Rigaku SmartLab system using  $\text{CuK}\alpha$  radiation. Differential scanning calorimetry (DSC) data were recorded on a Shimadzu DSC-60 plus (heating rate: 10  $^\circ\text{C min}^{-1}$ ). The intensity of the mechanical stimuli was measured by using a digital force gauge (IMADA, ZTA-500N).

[1] D. Rosario-Amorin, E. N. Duesler, R. T. Paine, B. P. Hay, L. H. Delmau, S. D. Reilly, A. J. Gaunt, B. L. Scott, *Inorg. Chem.* **2012**, *51*, 6667–6681.

## 2. Preparation of dibenzofuran-based bis(1-pyrenylmethyl)diamine 1

### 4,6-Bis(azidomethyl)dibenzo[*b,d*]furan (3)

To a stirred solution of dibenzo[*b,d*]furan-4,6-diyl dimethanol (**2**) (0.91 g, 4.0 mmol) and triphenylphosphine (2.6 g, 10 mmol) in THF (90 mL), an toluene solution (1.9 M) of diethyl azodicarboxylate (5.3 mL, 10 mmol) was added dropwise through a syringe at  $-20\text{ }^{\circ}\text{C}$ . After the reaction mixture was stirred at  $-20\text{ }^{\circ}\text{C}$  for 10 min, diphenylphosphoryl azide (2.2 mL, 10 mmol) was added dropwise to the mixture through a syringe. The reaction mixture was stirred at  $-20\text{ }^{\circ}\text{C}$  for 26 h, and then the solvent was removed under reduced pressure. Crude product was purified by silica-gel column chromatography twice (Silica gel 60N, hexane/ $\text{CH}_2\text{Cl}_2$ /AcOEt = 5:1:1 then toluene) to give **3** (0.64 g, 59%) as a white solid.

White solid; M.p. 56.2–57.2  $^{\circ}\text{C}$ ; IR (KBr):  $\nu_{\text{max}}$  2924, 2104, 1432, 1419, 1283, 1253, 1187, 1061, 875, 806, 780, 745  $\text{cm}^{-1}$ ;  $^1\text{H}$  NMR (500 MHz,  $\text{CDCl}_3$ ):  $\delta$  (ppm) 7.95 (dd,  $J = 7.6, 1.3$  Hz, 2H), 7.44 (dd,  $J = 7.6, 1.3$  Hz, 2H), 7.38 (t,  $J = 7.6$  Hz, 2H), 4.76 (s, 4H);  $^{13}\text{C}$  NMR (126 MHz,  $\text{CDCl}_3$ ):  $\delta$  (ppm) 154.2, 127.4, 124.5, 123.3, 121.1, 119.9, 49.5; HRMS-FAB ( $m/z$ ):  $[\text{M}]^+$  Calcd for  $\text{C}_{14}\text{H}_{10}\text{N}_6\text{O}$ , 278.0916, Found, 278.0916.

### Dibenzo[*b,d*]furan-4,6-diyl dimethanamine (4)

To a stirred solution of **3** (0.51 g, 1.9 mmol) in EtOAc (12 mL) was added 5% Pd/C (77 mg, 15 wt%) and the mixture was stirred under  $\text{H}_2$  atmosphere (1 atm balloon) at room temperature for 21 h. The reaction mixture was filtered through Celite to remove Pd/C. After the filtrate was concentrated under reduced pressure, **4** (0.33 g, 77%) was obtained as a white solid.

White solid; M.p. 120.1–123.1  $^{\circ}\text{C}$ ; IR (KBr):  $\nu_{\text{max}}$  3290, 3059, 2922, 1579, 1489, 1434, 1418, 1374, 1304, 1189, 1057, 771, 743  $\text{cm}^{-1}$ ;  $^1\text{H}$  NMR (500 MHz,  $\text{CDCl}_3$ ):  $\delta$  (ppm) 7.80 (dd,  $J = 7.5, 1.3$  Hz, 2H), 7.38–7.36 (m, 2H), 7.31–7.26 (m, 2H), 4.21 (s, 4H), 1.69 (br s, 4H);  $^{13}\text{C}$  NMR (126 MHz,  $\text{CDCl}_3$ ):  $\delta$  (ppm) 153.9, 127.4, 125.6, 124.2, 122.9, 119.2, 41.4; HRMS-ESI ( $m/z$ ):  $[\text{M}+\text{H}]^+$  Calcd for  $\text{C}_{14}\text{H}_{15}\text{N}_2\text{O}$ , 227.1179, Found, 227.1166.

### *N,N'*-[Dibenzo[*b,d*]furan-4,6-diylbis(methylene)]bis(2-nitrobenzenesulfonamide) (5)

To a stirred solution of **4** (80 mg, 0.35 mmol) and  $\text{Et}_3\text{N}$  (0.20 mL, 1.4 mmol) in THF (5.0 mL) was added dropwise a solution of  $\text{NsCl}$  (0.19 g, 0.84 mmol) in THF (9.0 mL) at  $0\text{ }^{\circ}\text{C}$  and the mixture was stirred at room temperature for 22 h. Water and  $\text{CH}_2\text{Cl}_2$  were added to the reaction mixture. The organic layer was separated, and the aqueous layer was extracted three times with  $\text{CH}_2\text{Cl}_2$ . The combined organic layer was washed with water and brine, dried over anhydrous  $\text{Na}_2\text{SO}_4$ , and filtered. After removal of the solvent under reduced pressure, the crude product was purified by silica-gel column chromatography (Silica gel 60N,  $\text{CH}_2\text{Cl}_2$ ) to give **5** (0.12 g, 59%) as a white solid.

White solid; M.p. 195.4–196.1 °C; IR (KBr):  $\nu_{\max}$  3334, 3095, 1539, 1417, 1368, 1340, 1162, 1124, 1061, 854, 770, 737  $\text{cm}^{-1}$ ;  $^1\text{H}$  NMR (500 MHz, DMSO- $d_6$ ):  $\delta$  (ppm) 8.76 (br s, 2H), 7.91 (d,  $J = 7.6$  Hz, 2H), 7.82 (dd,  $J = 7.7, 0.9$  Hz, 2H), 7.80 (dd,  $J = 7.7, 0.9$  Hz, 2H), 7.64 (td,  $J = 7.7, 0.9$  Hz, 2H), 7.53 (td,  $J = 7.7, 0.9$  Hz, 2H), 7.41 (d,  $J = 7.6$  Hz, 2H), 7.27 (t,  $J = 7.6$  Hz, 2H); 4.58 (s, 4H);  $^{13}\text{C}$  NMR (126 MHz, DMSO- $d_6$ ):  $\delta$  (ppm) 152.8, 147.2, 133.7, 133.0, 132.1, 129.2, 126.8, 124.1, 123.2, 123.0, 121.0, 120.3, 40.9; HRMS-ESI ( $m/z$ ):  $[\text{M}+\text{H}]^+$  Calcd for  $\text{C}_{26}\text{H}_{21}\text{N}_4\text{O}_9\text{S}_2$ , 597.0745, Found, 597.0771.

*N,N'*-[Dibenzo[*b,d*]furan-4,6-diylbis(methylene)]bis[2-nitro-*N*-(pyren-1-ylmethyl)benzenesulfonamide] (6)

To a stirred solution of **5** (0.15 g, 0.25 mmol) in DMF (10 mL) was added  $\text{K}_2\text{CO}_3$  (0.20 g, 1.5 mmol) and 1-(bromomethyl)pyrene (0.17 g, 0.59 mmol). After the mixture was stirred at 60 °C for 1.5 h, water and  $\text{CH}_2\text{Cl}_2$  were added to the mixture. The organic layer was separated, and the aqueous layer was extracted three times with  $\text{CH}_2\text{Cl}_2$ . The combined organic layer was washed with water and brine, dried over anhydrous  $\text{Na}_2\text{SO}_4$ , and filtered. After removal of the solvent under reduced pressure, the crude product was purified by silica-gel column chromatography (Silica gel 60N,  $\text{CH}_2\text{Cl}_2$ ) to give **6** (0.25 g, 98%) as a yellow solid.

Yellow solid; M.p. 160.9–163.4 °C; IR (KBr):  $\nu_{\max}$  3041, 1542, 1436, 1418, 1350, 1162, 1124, 913, 849, 772  $\text{cm}^{-1}$ ;  $^1\text{H}$  NMR (500 MHz,  $\text{CDCl}_3$ ):  $\delta$  (ppm) 8.00 (dd,  $J = 5.9, 2.6$  Hz, 2H), 7.85–7.81 (m, 6H), 7.67 (d,  $J = 9.0$  Hz, 2H), 7.61 (d,  $J = 9.0$  Hz, 2H), 7.56–7.50 (m, 10H), 7.37–7.32 (m, 4H), 7.17 (td,  $J = 7.6, 1.3$  Hz, 2H), 7.06 (d,  $J = 7.6$  Hz, 2H), 6.90 (t,  $J = 7.6$  Hz, 2H), 5.00 (s, 4H), 4.36 (s, 4H);  $^{13}\text{C}$  NMR (126 MHz,  $\text{CDCl}_3$ ):  $\delta$  (ppm) 153.2, 147.7, 133.7, 133.0, 131.3, 130.8, 130.3, 130.2, 129.0, 127.6, 127.4, 127.3, 127.1, 126.93, 126.91, 125.7, 125.1, 125.0, 124.18, 124.14, 124.0, 123.5, 122.7, 121.7, 119.5, 119.3, 49.5, 45.5 (two signals are hidden due to the incidental overlapping); HRMS-FAB ( $m/z$ ):  $[\text{M}]^+$  Calcd for  $\text{C}_{60}\text{H}_{40}\text{N}_4\text{O}_9\text{S}_2$ , 1024.2237, Found, 1024.2240.

*1,1'*-(Dibenzo[*b,d*]furan-4,6-diyl)bis[*N*-(pyren-1-ylmethyl)methanamine] (1)

To a stirred solution of PhSH (0.51 mL, 4.5 mmol) in  $\text{CH}_3\text{CN}$  (20 mL) was added dropwise an aqueous solution of KOH (11 M, 0.45 mL, 5.0 mmol) at 0 °C and the mixture was stirred for 5 min. To the mixture was added a solution of **6** (1.0 g, 1.0 mmol) in  $\text{CH}_3\text{CN}$  (90 mL) at room temperature. After the mixture was stirred at 50 °C for 45 min, water and  $\text{CH}_2\text{Cl}_2$  were added to the mixture. The organic layer was separated, and the aqueous layer was extracted three times with  $\text{CH}_2\text{Cl}_2$ . The combined organic layer was washed with water and brine, dried over anhydrous  $\text{Na}_2\text{SO}_4$ , and filtered. After removal of the solvent under reduced pressure, the crude product was purified by recrystallization from hot toluene to give **1** (0.47 g, 74%) as a white solid.

White solid; M.p. 170.9–172.1 °C; IR (KBr):  $\nu_{\max}$  3294, 3041, 2830, 1603, 1587, 1431, 1306, 1189, 1109, 1094, 1004, 966, 846, 764  $\text{cm}^{-1}$ ;  $^1\text{H}$  NMR (500 MHz,  $\text{CDCl}_3$ ):  $\delta$  (ppm) 8.13 (d,  $J = 9.1$  Hz, 2H), 8.07–8.04

(m, 4H), 7.96 (d,  $J = 7.6$  Hz, 2H), 7.93–7.86 (m, 12H), 7.50 (d,  $J = 7.5$  Hz, 2H), 7.36 (t,  $J = 7.5$  Hz, 2H), 4.37 (s, 4H), 4.23 (s, 4H), 1.97 (br s, 2H);  $^{13}\text{C}$  NMR (126 MHz,  $\text{CDCl}_3$ ):  $\delta$  (ppm) 154.5, 133.5, 131.1, 130.7, 130.5, 129.0, 127.4, 127.3, 127.2, 126.9 (2C), 125.7, 124.9, 124.84, 124.83, 124.7, 124.5, 124.4, 124.3, 123.0, 122.9, 119.5, 50.9, 48.1; HRMS-FAB ( $m/z$ ):  $[\text{M}+\text{H}]^+$  Calcd for  $\text{C}_{48}\text{H}_{35}\text{N}_2\text{O}$ , 655.2749, Found, 655.2763.

### 3. Preparation of two-component dyes

A 1:1 molar amount of **1** (0.015 mmol, 10 mg) and **DMQA** (0.015 mmol, 5.2 mg) was mixed in  $\text{CH}_2\text{Cl}_2$  (3.0 mL), and the solvent was evaporated under reduced pressure (ca. 70 hPa, 30 °C, 4 min). The residue was heated on a hotplate to 140 °C and cooled to room temperature. The resulting mixture is referred to as as-prepared **1/DMQA**. The two-component mixtures of **1/FS**, **1/PTCDI**, **1/PER**, and **1/AQ** were also prepared by the same procedure.

#### 4. Repeated MCL of 1 and two-component dyes

The maximum emission wavelengths of heated and ground samples were recorded within experimental errors during five grinding–heating cycles for the MCL of **1**, **1/DMQA**, and **1/PTCDI** (Figure S1a–c). The MCL of **1/AQ** was also reversible at least five cycles between heated and gently ground states as well as between heated and strongly ground states (Figure S1d and S1e).

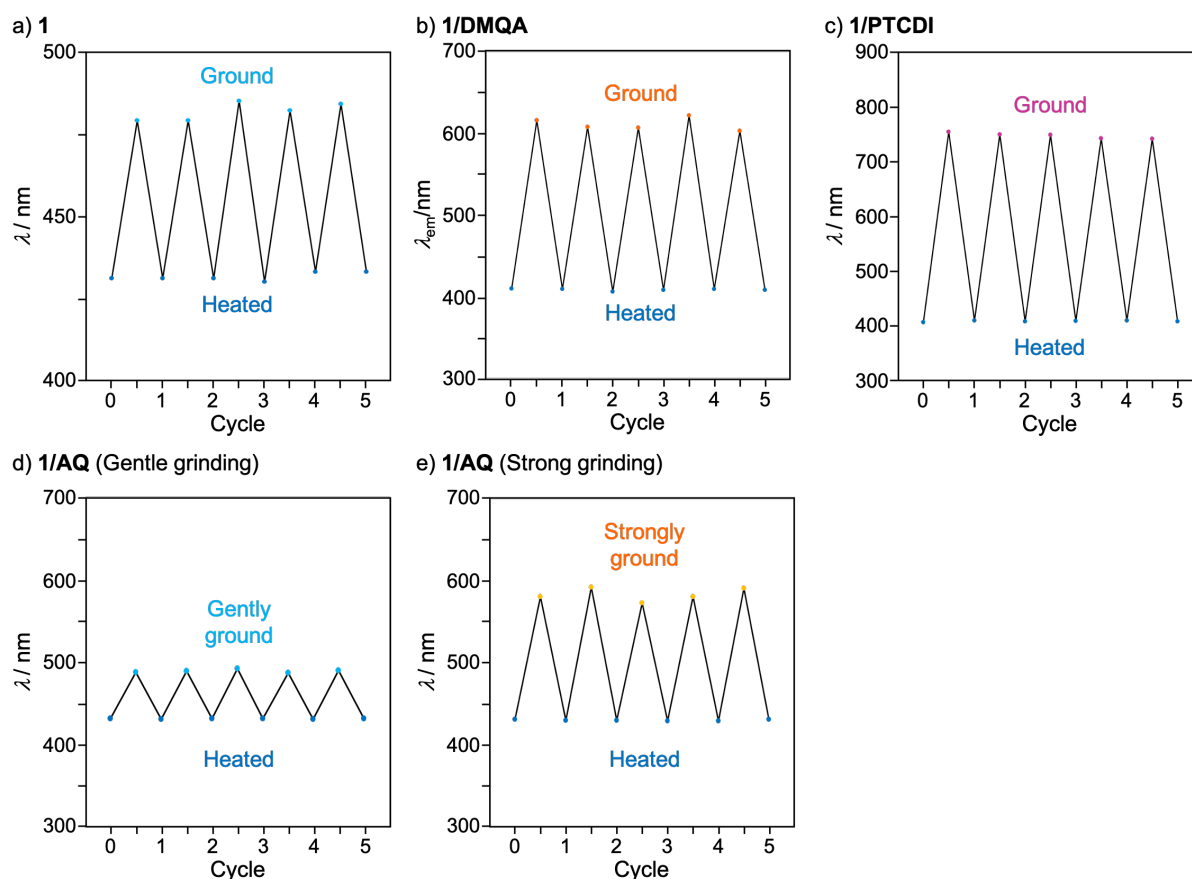


**Figure S1** Plots of the maximum emission wavelengths during five grinding–heating cycles. a) MCL between ground and heated **1**. b) MCL between ground and heated **1/DMQA**. c) MCL between ground and heated **1/PTCDI**. d) MCL between gently ground and heated **1/AQ**. e) MCL between strongly ground and heated **1/AQ**.

## 5. Solid-state emission properties of organic dyes

Under irradiation of UV light (365 nm), powdered samples of **DMQA**, **PER**, and **AQ** exhibited weak orange, yellow, and weak yellow-green emission, respectively (Figure S2a, S2d, and S2e). Powdered samples of **FS** and **PTCDI** were non-emissive (Figure S2b and S2c). The emission properties of these dyes almost unchanged after grinding with a spatula.

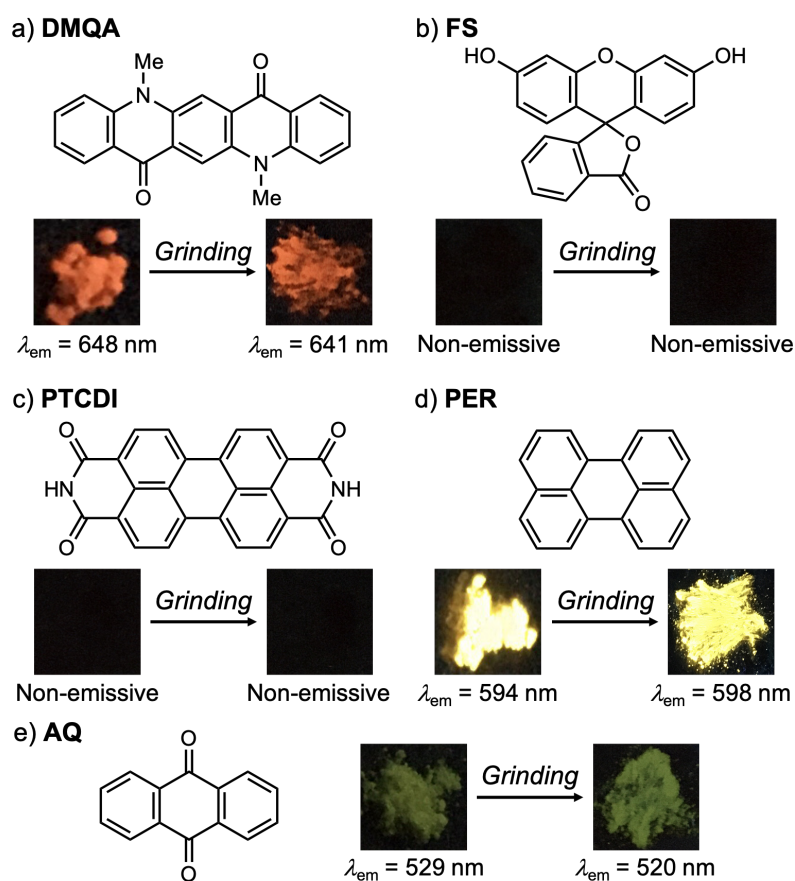


**Figure S2** Photograph of crystalline and ground samples of organic dyes under UV light ( $\lambda_{ex} = 365$  nm). a) **DMQA**, b) **FS**, c) **PTCDI**, d) **PER**, e) **AQ**.

Although the emission properties of **DMQA**, **FS**, **PTCDI**, **PER**, and **AQ** unchanged after grinding (Figure S2), these crystalline dyes changed to amorphous states upon grinding (Figure S3).

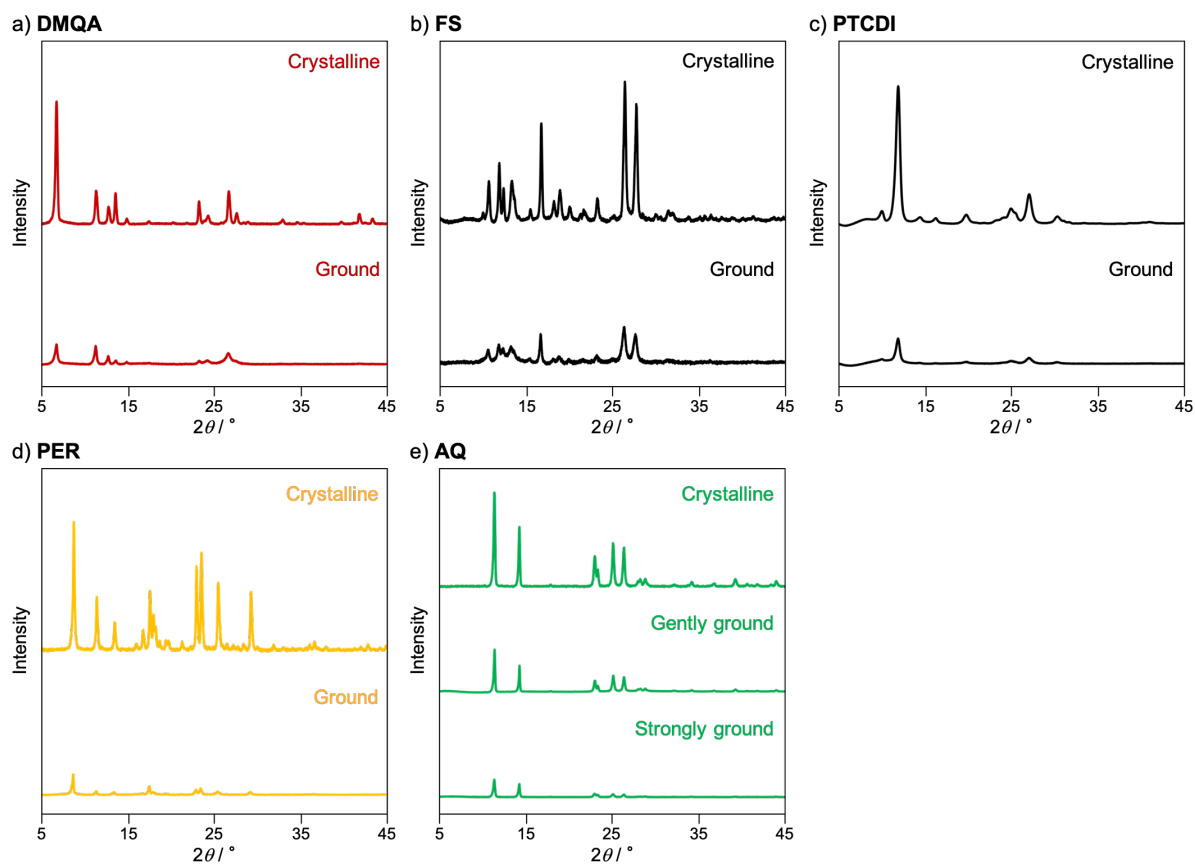


**Figure S3** PXRD patterns for the crystalline and ground samples of a) **DMQA**, b) **FS**, c) **PTCDI**, and d) **PER**. e) PXRD patterns for the crystalline, gently ground, and strongly ground samples of **AQ**.

## 6. Applicability of other preparation methods

The MCL property of **1/DMQA** was independent of the evaporation rate and the solvent used for the preparation. When the bath temperature for evaporation was set at 15 °C and 50 °C, the evaporation of solvent was completed in 9 min and 1.5 min, respectively, at about 70 hPa. After heating the residue to 140 °C and cooled to room temperature, the resulting **1/DMQA** exhibited the same MCL properties as that prepared by the general method (Figure S4a and S4b). When MeOH, CHCl<sub>3</sub>, AcOEt, or toluene was used as the solvent instead of CH<sub>2</sub>Cl<sub>2</sub>, the resulting **1/DMQA** also exhibited the same MCL properties as that prepared by using CH<sub>2</sub>Cl<sub>2</sub> (Figure S4c–f).

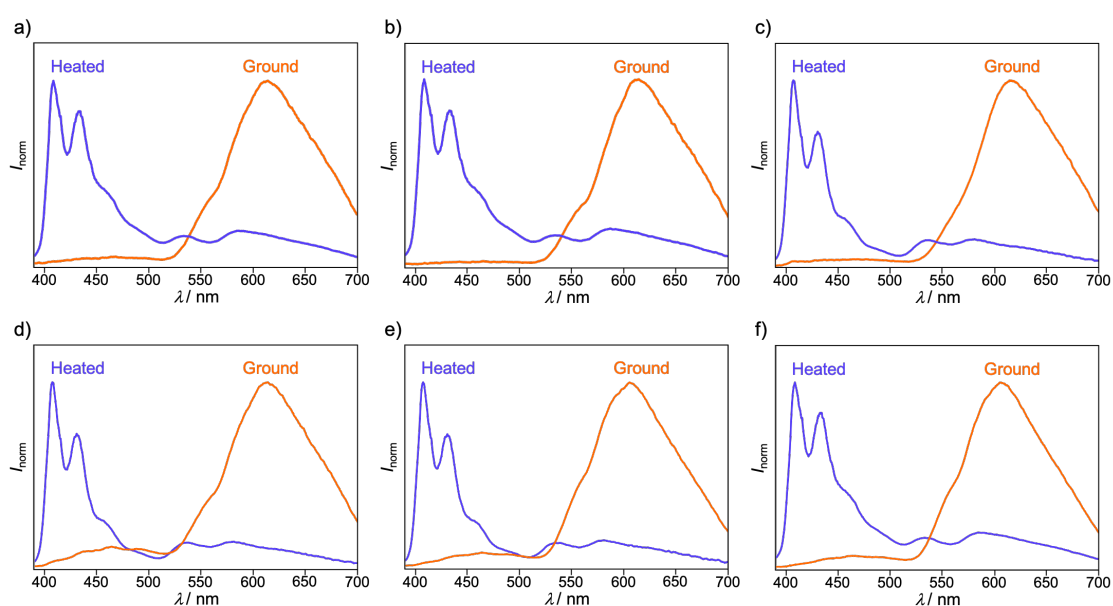


**Figure S4** Fluorescence spectra for the MCL of **1/DMQA** prepared by different conditions. Evaporation conditions (ca. 70 hPa): a) 15 °C, 9 min, b) 50 °C, 1.5 min, c–f) 30 °C, 4 min. Solvent: a,b) CH<sub>2</sub>Cl<sub>2</sub>, c) MeOH, d) CHCl<sub>3</sub>, e) AcOEt, f) toluene.

## 7. Mechanochromic luminescence (MCL) of two-component dyes

### 7.1. Fluorescence spectra

Wide-range MCL was achieved for **1/DMQA** and **1/FS**, whereas a relatively narrower shift in the maximum emission wavelength was observed in the MCL of **1/PER** (Figure S5).

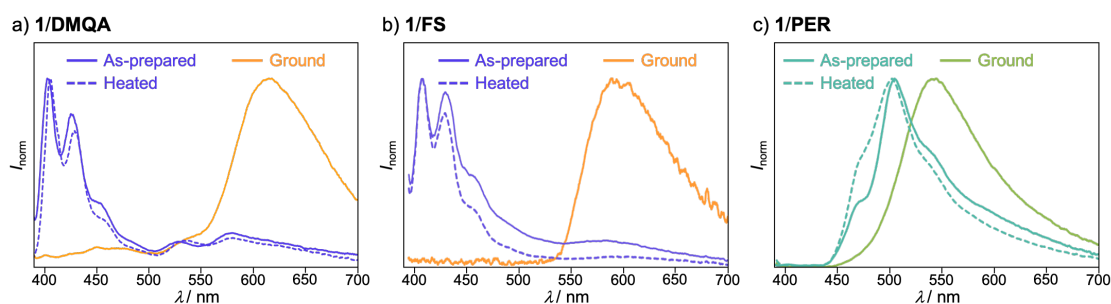


**Figure S5** Fluorescence spectra for the MCL of a) **1/DMQA**, b) **1/FS**, and c) **1/PER**.

### 7.2. PXRD patterns

The diffraction peaks of as-prepared **1/FS**, **1/PTCDI**, and **1/AQ** corresponded to a superposition of those of **1** and the acceptor dye (Figure S6a, S6b, and S6d). On the other hand, the diffraction patterns of **PER** were not observed in the PXRD analysis of as-prepared **1/PER** (Figure S6c).

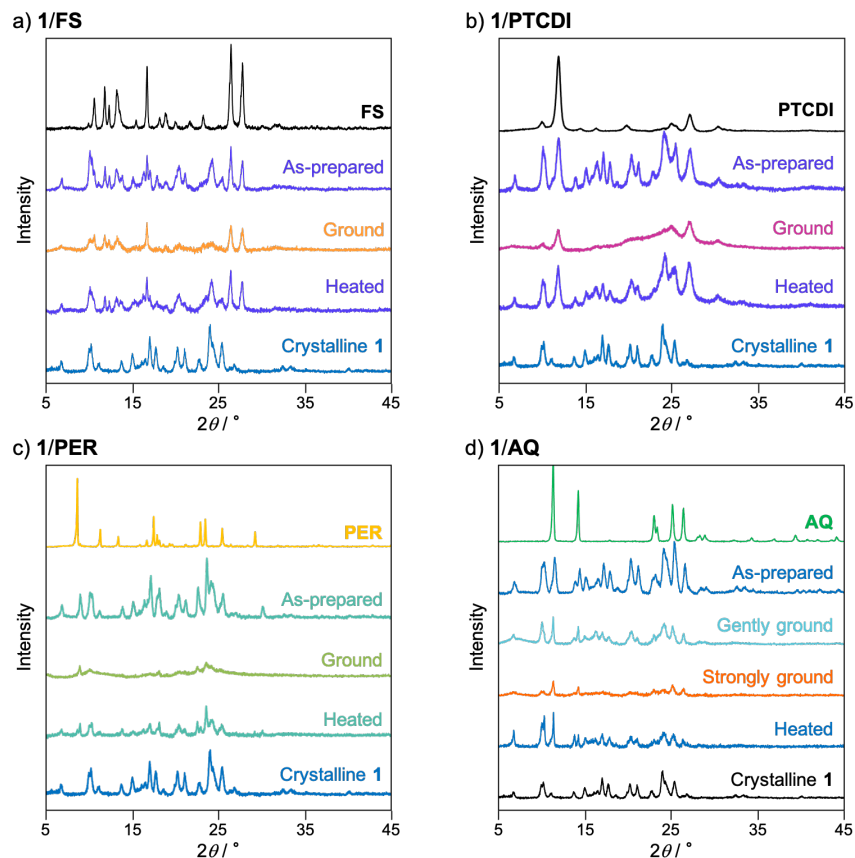


**Figure S6** PXRD patterns for the MCL of a) **1/FS**, b) **1/PTCDI**, c) **1/PER**, and d) **1/AQ**.

### 7.3. DSC thermograms

Only one endothermic peak was observed in the DSC thermograms of as-prepared two-component dyes **1/FS**, **1/PTCDI**, **1/PER**, and **1/AQ** (Figure S7). Gently ground **1/AQ** also exhibited only one endothermic peak (Figure S7d). Broad cold-crystallization transition peaks followed by endothermic melting peaks were detected in the DSC thermograms of the two-component dyes after grinding (Figure S7).

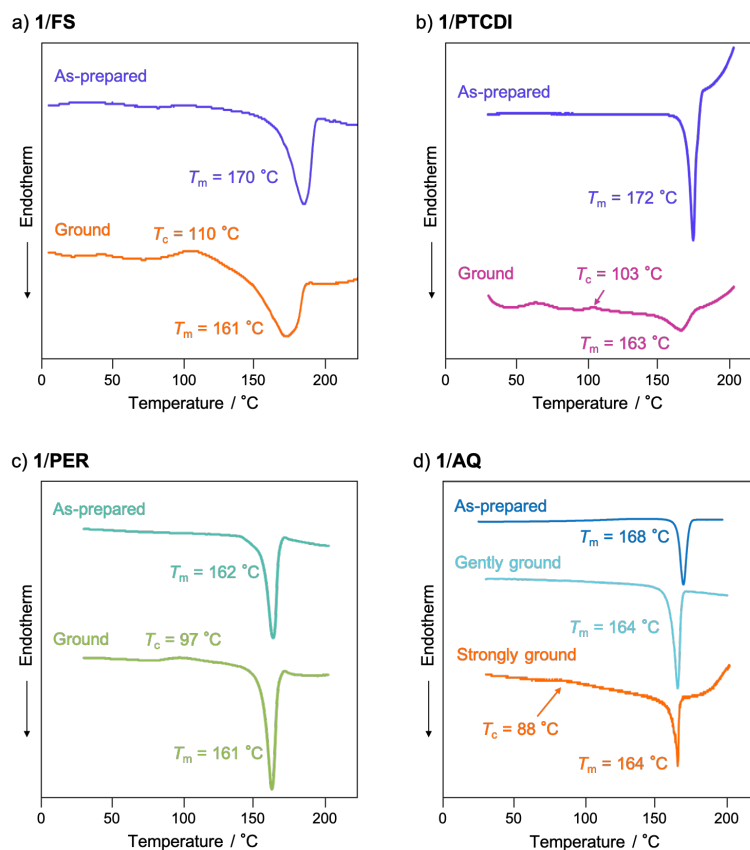


**Figure S7** DSC thermograms for the MCL of a) **1/FS**, b) **1/PTCDI**, c) **1/PER**, and d) **1/AQ**.

#### 7.4. Properties of reground samples

The reground samples of the two-component dyes exhibited almost the same fluorescence spectra, PXRD patterns, and DSC thermograms as those of initially ground samples (Figure S8–10).

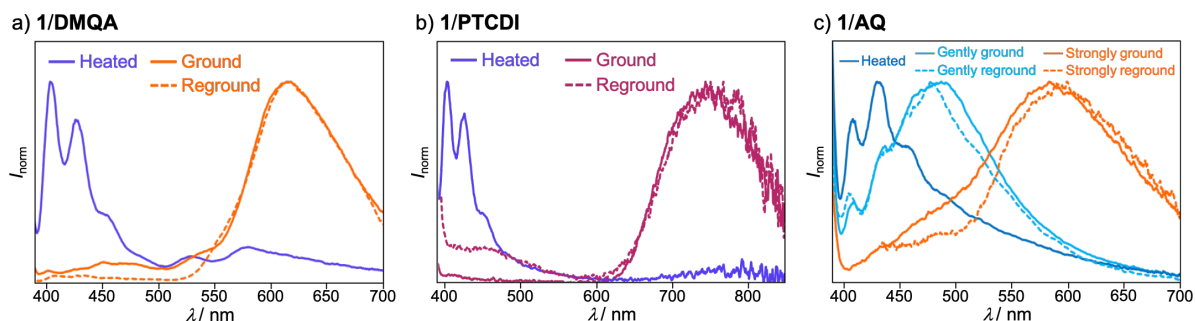


**Figure S8** Fluorescence spectra for the heated, ground, and reground samples of a) 1/DMQA, b) 1/PTCDI, and c) 1/AQ.

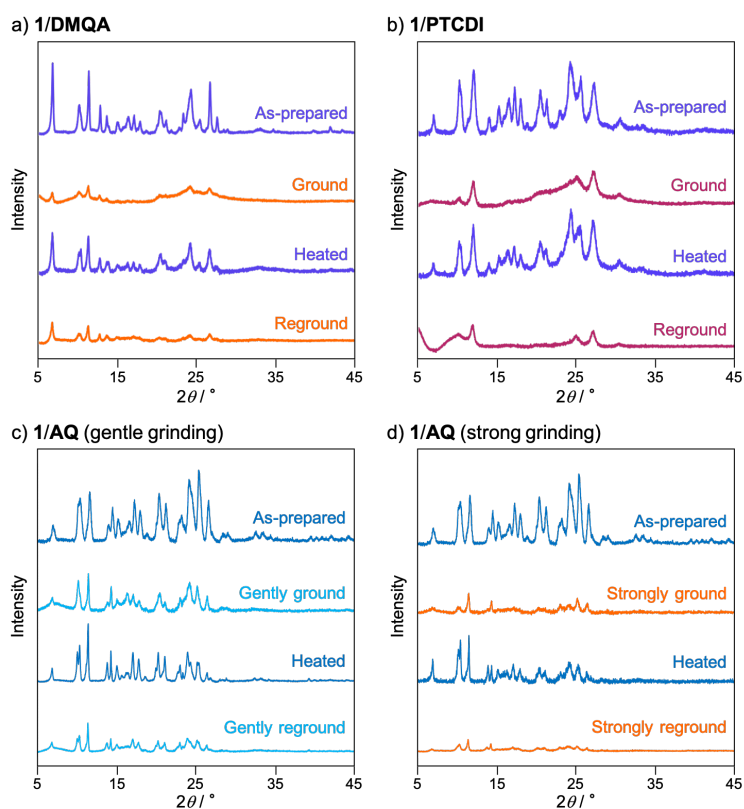


**Figure S9** PXRD patterns for the as-prepared, ground, heated, and reground samples of a) 1/DMQA and b) 1/PTCDI. c) PXRD patterns for the as-prepared, gently ground, heated, and gently reground samples of 1/AQ. d) PXRD patterns for the as-prepared, strongly ground, heated, and strongly reground samples of 1/AQ.

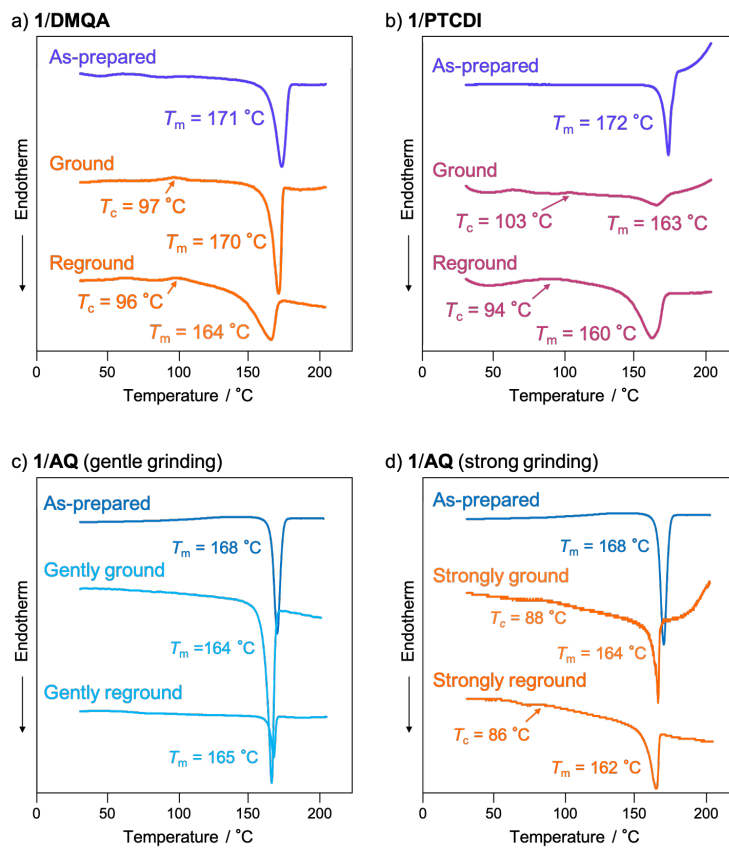


**Figure S10** DSC thermograms for the as-prepared, ground, and reground samples of a) **1/DMQA** and b) **1/PTCDI**. c) DSC thermograms for the as-prepared, gently ground, and gently reground samples of **1/AQ**. d) DSC thermograms for the as-prepared, strongly ground, and strongly reground samples of **1/AQ**.

## 8. Single-particle-level observations by fluorescence microscopy

Single-particle fluorescence measurements were performed on a home-built wide-field/confocal microscope equipped with a Nikon Ti-E inverted fluorescence microscope. The fluorescence images were recorded using a color sCMOS camera (Dhyana 400DC, Tucson Photonics). The 405-nm continuous wave laser (OBIS 405LX, Coherent) or 405-nm pulsed diode laser (PiL040X, Advanced Laser Diode System, 45-ps FWHM) was used to excite the samples. A dichroic mirror (Di02-R405, Semrock) and a longpass filter (ET425lp, Chroma) were used to filter the scattering from excitation light. To separate the fluorescence signals, bandpass filters (FF01-375/110, FF01-535/50, FF01-731/137, Semrock) were used. An area of approximately  $1 \mu\text{m}^2$  on a target particle or region was spatially selected using a 100- $\mu\text{m}$  pinhole to measure its spectrum and fluorescence lifetime. For the spectroscopy, only the emission that passed through the pinhole and a slit entered the imaging spectrograph (MS3504i, SOL instruments) equipped with a CCD camera (DU416A-LDC-DD, Andor). For time-resolved fluorescence measurements, the emitted photons were passed through the pinhole and then directed onto a single-photon avalanche diode (SPD-050, Micro Photon Devices). The signals from the detector were sent to a time-correlated single photon counting module (SPC-130EM, Becker & Hickl) for further analysis. The instrument response function of the system was about 100 ps. All the experiments were conducted at room temperature. The data were analyzed using ImageJ (<http://rsb.info.nih.gov/ij/>) and Origin 2021 (OriginLab).

---

### 8.1. Single-particle-level observations of **1** and **PTCDI**

Blue-emissive crystals and red-emissive crystals were observed for crystalline **1** and **PTCDI**, respectively, under the fluorescence microscope (Figure S11a and S11b). Fluorescence spectra of crystalline **1** and **PTCDI** were in good agreement with those of blue-emissive and red-emissive regions of as-prepared **1/PTCDI**, respectively (Figure S11d). Since a high numerical aperture objective lens used for the microscope measurements lens effectively collects the emitted photons from the focal plane (i.e., the crystal surface), green emission from minor amorphous regions is more prominent compared with the bulk sample. Although the morphology of **PTCDI** was changed after grinding, the emission band of ground **PTCDI** was observed at the same wavelength region as that of crystalline **PTCDI**. The emission band of ground **PTCDI** was in good agreement with that of ground **1/PTCDI** (Figure S11c and S11e).

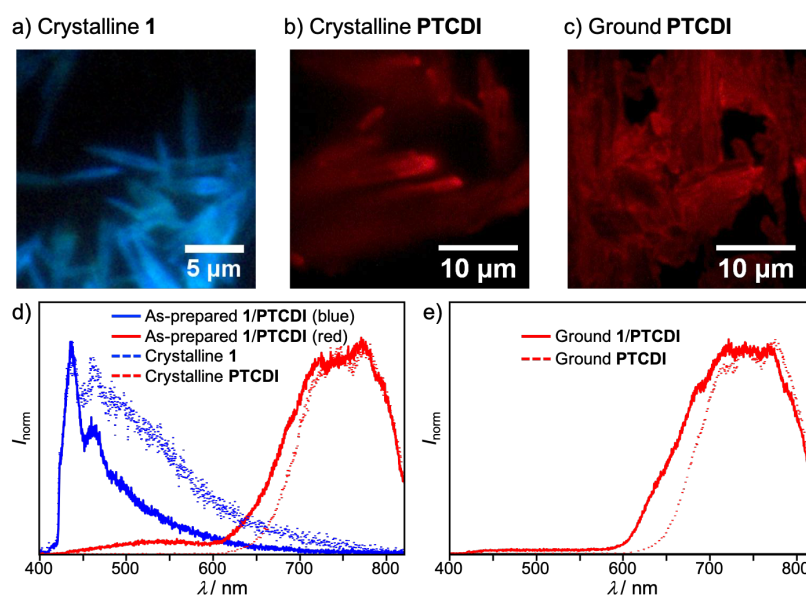


**Figure S11** Photographs and fluorescence spectra recorded at the single-particle level with excitation wavelength of 405 nm. Photographs of a) crystalline **1**, b) crystalline **PTCDI**, and c) ground **PTCDI**. d) Fluorescence spectra of as-prepared **1/PTCDI** (blue and red lines), crystalline **1** (blue dotted line), and crystalline **PTCDI** (red dotted line). e) Fluorescence spectra of ground **1/PTCDI** (red line) and ground **PTCDI** (red dotted line).

## 8.2. Single-particle-level observations of ground samples of 1/PTCDI and 1

Although blue emission was observed for the heated 1/PTCDI in the bulk state, green and red-emissive regions were also observed in the single-particle-level observation of heated 1/PTCDI (Figure S12a). The emission spectrum of the green-emissive region of 1/PTCDI was in good agreement with that of ground 1, indicating that the green-emissive region of heated 1/PTCDI should exist in an amorphous state (Figure S12b and S12c).

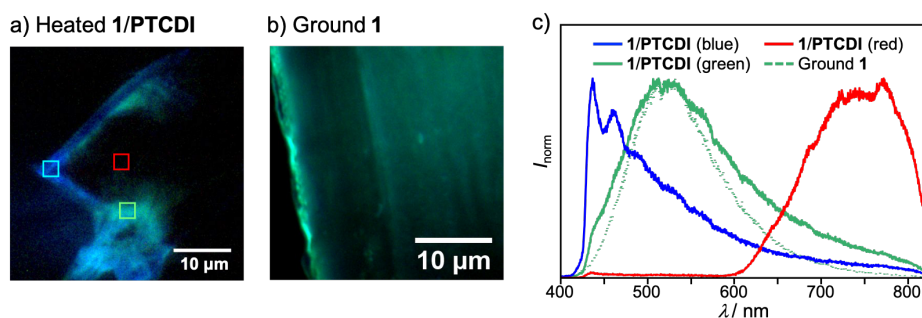


**Figure S12** a) Photograph of heated 1/PTCDI, b) photograph of ground 1, and c) fluorescence spectra of heated 1/PTCDI (blue, green, and red lines) and ground 1 (green dotted line) recorded at the single-particle level ( $\lambda_{\text{ex}} = 405$  nm). The square marks in indicate the measured locations.

## 8.3. Fluorescence lifetimes of crystalline and ground 1

Both blue-emissive crystalline 1 and green-emissive ground 1 exhibited two components ( $\tau_1$  and  $\tau_2$ ) in the blue and green region, respectively (Table S1). The mean fluorescence lifetime ( $\langle\tau\rangle$ ) of ground 1 was longer than that of crystalline 1.

**Table S1.** The fluorescence decay times for crystalline and ground 1

| Sample        | Region (nm) | $\tau_1$ (ns) <sup>[a]</sup> | $\tau_2$ (ns) <sup>[a]</sup> | $\langle\tau\rangle$ (ns) <sup>[b]</sup> |
|---------------|-------------|------------------------------|------------------------------|--|
| Crystalline 1 | 417–430     | 0.36 (0.87)                  | 3.32 (0.14)                  | 2.1                                      |
| Ground 1      | 510–560     | 0.40 (0.67)                  | 4.67 (0.24)                  | 3.8                                      |

[a] The coefficient  $a_n$  of the component is shown in parentheses.

[b] Intensity-weighted mean fluorescence lifetime.  $\langle\tau\rangle = (a_1\tau_1^2 + a_2\tau_2^2)/(a_1\tau_1 + a_2\tau_2)$ .

#### 8.4. Single-particle-level observations of heated and ground samples of **1/DMQA** and **1/FS**

Segregated crystals that exhibit strong blue and weak orange emission were observed for the heated samples of **1/DMQA** and **1/FS**, because crystalline **DMQA** and **FS** are almost nonemissive due to the concentration quenching. Homogeneous orange emission was observed for the ground samples of **1/DMQA** and **1/FS** (Figure S13).

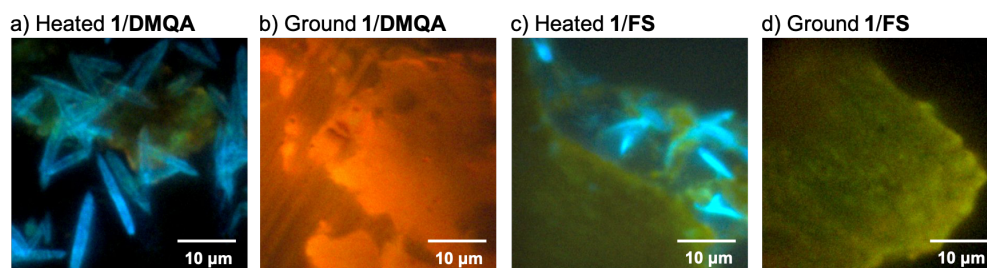


**Figure S13** Photographs of a) heated **1/DMQA**, b) ground **1/DMQA**, c) heated **1/FS**, and d) ground **1/FS** recorded at the single-particle level ( $\lambda_{\text{ex}} = 405 \text{ nm}$ ).

### 9. Measurement of the intensity of mechanical stimuli

The intensity of the mechanical stimuli required for the emission-color change in the two-step MCL of **1/AQ** and bicolor MCL of **1** was measured by using a digital force gauge (Table S2). With a flat circular contact surface (diameter: 1.0 cm) in contact with the sample, the pressure applied to the contact surface by manual grinding was monitored. The grinding force was gradually increased, and the pressure at which the luminescence color changed was recorded. Five experiments were conducted, and the average value was calculated. The second step of the two-step MCL of **1/AQ** required about twice the intensity of the stimulus compared to the first step. Meanwhile, the intensity of the stimulus required for the emission-color change of **1** was almost the same as that required for the first step emission-color change of **1/AQ**.

**Table S2.** The intensity of mechanical stimuli required for the emission-color switching in the two-step MCL of **1/AQ** and bicolor MCL of **1**

| Sample                    | Run 1<br>(N cm <sup>-2</sup> ) | Run 2<br>(N cm <sup>-2</sup> ) | Run 3<br>(N cm <sup>-2</sup> ) | Run 4<br>(N cm <sup>-2</sup> ) | Run 5<br>(N cm <sup>-2</sup> ) | Average<br>(N cm <sup>-2</sup> ) |
|---------------------------|--------------------------------|--------------------------------|--------------------------------|--------------------------------|--------------------------------|----------------------------------|
| <b>1/AQ</b> (first step)  | 5.5                            | 3.9                            | 5.6                            | 5.5                            | 4.6                            | 5.0                              |
| <b>1/AQ</b> (second step) | 9.6                            | 10.6                           | 12.0                           | 13.6                           | 10.4                           | 11.2                             |
| <b>1</b>                  | 5.5                            | 5.6                            | 4.8                            | 5.1                            | 5.6                            | 5.3                              |

## 10. Absorption properties

The absorption bands of **PER**, **FS**, and **PTCDI** were well overlapped with the fluorescence band of ground **1** (Figure S14a). The absorption spectra of two-component dyes **1/DMQA**, **1/FS**, **1/PTCDI**, and **1/PER**, as well as **1** almost unchanged after grinding (Figure S14b–f).

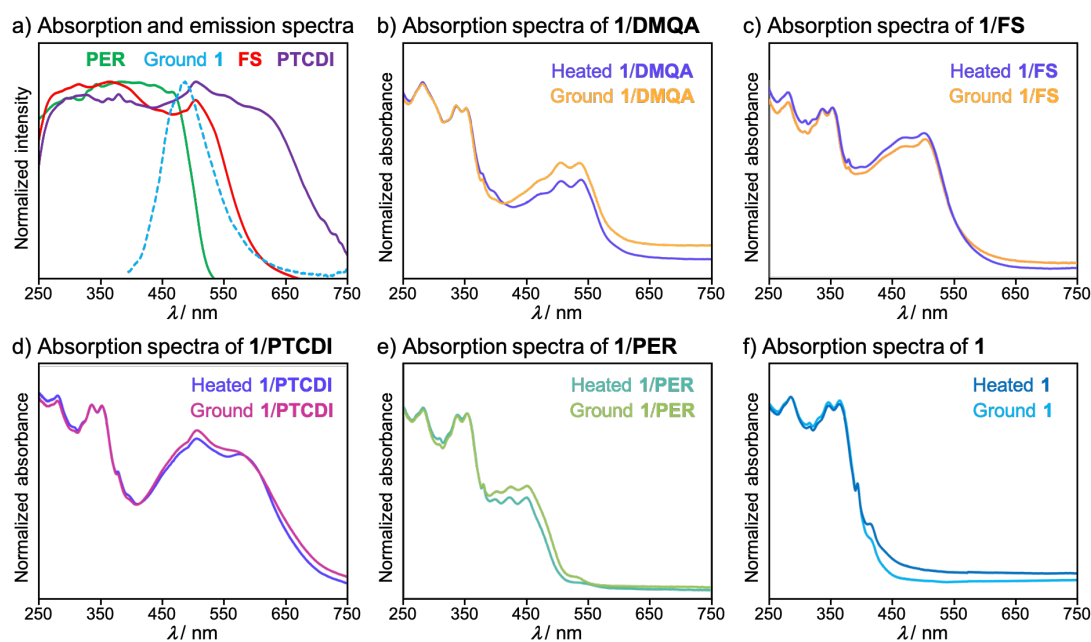


**Figure S14** a) Absorption spectra of organic dyes **PER**, **FS**, and **PTCDI** and fluorescence spectrum of ground **1**. b–f) Absorption spectra of heated and ground samples of b) **1/DMQA**, c) **1/FS**, d) **1/PTCDI**, e) **1/PER**, and f) **1**.

The color of **1/AQ** under room light was pale yellow for as-prepared and gently ground samples. After strong grinding, the color of **1/AQ** changed to yellow (Figure S15).

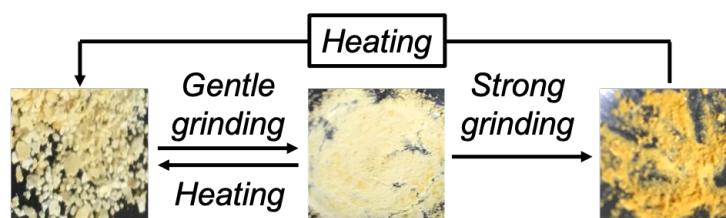


**Figure S15** Photographs for the two-step MCL of **1/AQ** under ambient light.

The absorption spectra of the reground samples of **1/AQ** showed that the CT band was observed after strong grinding (Figure S16).

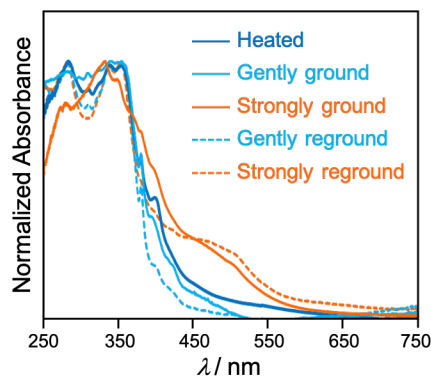


**Figure S16** Absorption spectra for the two-step MCL of **1/AQ**.

## 11. Proposed mechanism of the bicolor MCL

In contrast to **1/AQ** that exhibited two-step MCL, two-component dyes of **1** with FRET acceptors exhibited bicolor MCL. The gently ground state of the two-component dyes is a mixture of crystalline and amorphous **1** and acceptor dyes (Figure S17). Energy transfer should occur from amorphous **1** to both crystalline and amorphous acceptors. As a result, blue emission from crystalline **1** and FRET emission from acceptor dyes should be observed mainly from the gently ground samples.

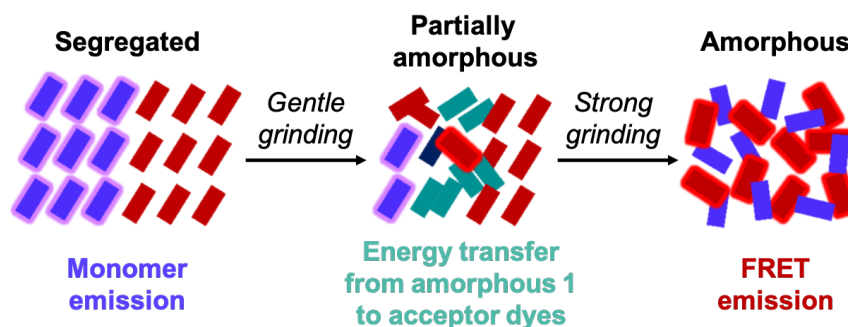


**Figure S17** Proposed mechanism for the bicolor MCL of **1** with acceptor dyes.

## 12. Solution-state studies

The fluorescence spectra of **1** and **1/DMQA** in chloroform solutions were recorded at different concentrations (Figure S18). The intensity of the excimer emission of **1** ( $\lambda_{em} = 478$  nm) at a concentration of  $1.0 \times 10^{-5}$  M slightly decreased by mixing with an equimolar amount of **DMQA** (Figure S18a). A more significant reduction of the emission intensity of **1** was observed for a  $1.0 \times 10^{-4}$  M solution of **1/DMQA** (Figure S18b). A solution of **1/DMQA** at  $1.0 \times 10^{-3}$  M in chloroform could not be prepared due to the low solubility of **DMQA**. The resulting suspension of **1/DMQA** in chloroform exhibited an almost complete reduction of the excimer emission of **1**. In this case, the emission intensity of **DMQA** was smaller than that observed from the  $1.0 \times 10^{-4}$  M solution probably due to the self-absorption (Figure S18c). The difference in the emission intensity of **1** in chloroform solutions of different concentrations is shown in Figure S18d.

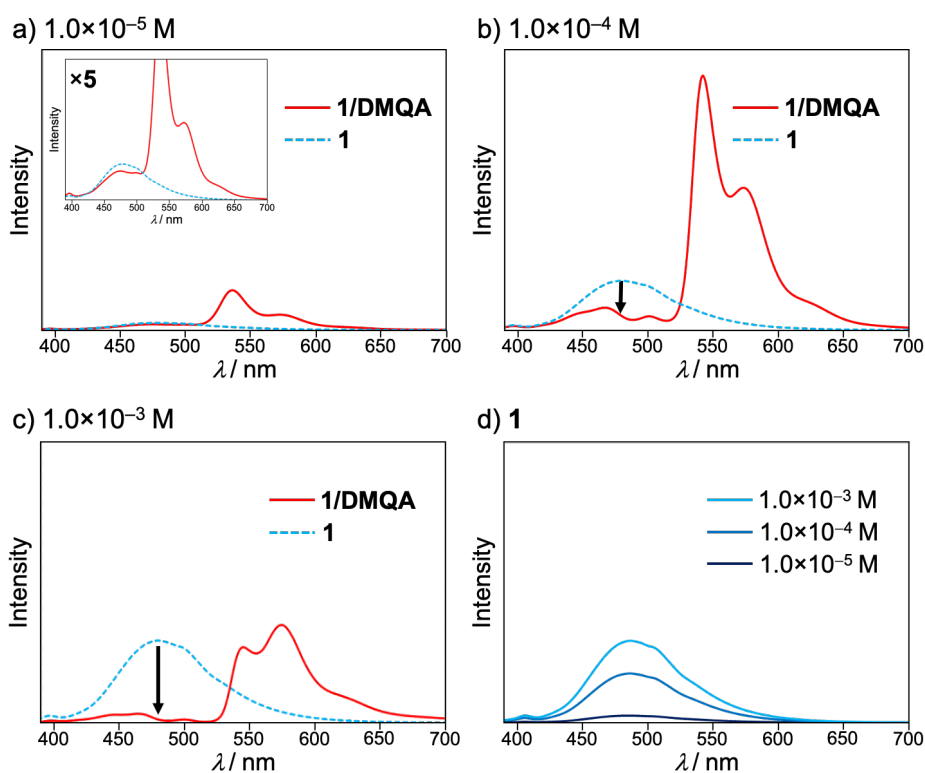


**Figure S18** Fluorescence spectra of **1** and **1/DMQA** in chloroform ( $\lambda_{ex} = 365$  nm). The vertical axis is set to the same scale. a) **1** and **1/DMQA** at  $1.0 \times 10^{-5}$  M, b) **1** and **1/DMQA** at  $1.0 \times 10^{-4}$  M, c) **1** and **1/DMQA** at  $1.0 \times 10^{-3}$  M. **DMQA** was not fully dissolved in chloroform at this concentration. d) **1** at  $1.0 \times 10^{-5}$  M,  $1.0 \times 10^{-4}$  M, and  $1.0 \times 10^{-3}$  M.

The intensity of the excimer emission of **1** in a DMF solution ( $5.0 \times 10^{-5}$  M) significantly decreased in the presence of **PTCDI** (Figure S19a). Although **PTCDI** was not fully dissolved in DMF, a suspension of **PTCDI** exhibited fluorescence at around 533 nm and 788 nm upon excitation at 487 nm that corresponds to the emission wavelength of the excimer emission of **1**. These emission bands should be assignable to the emission from monomer and aggregates of **PTCDI**, respectively. When the insoluble **PTCDI** aggregates were removed by filtration using a membrane filter, the emission band in the long wavelength region was not observed (Figure S19b).

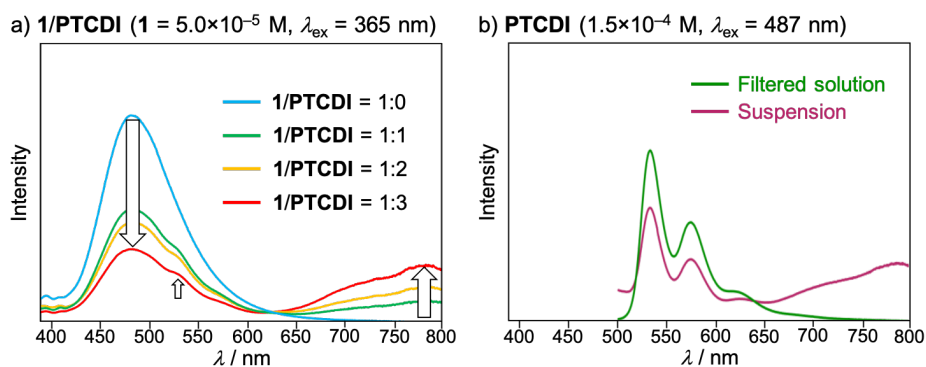


**Figure S19** Fluorescence spectra of a) **1**/PTCDI and b) PTCDI in DMF.

The absorption spectra of **1** in chloroform solutions ( $1 = 5.0 \times 10^{-3} \text{ M}$ ) were recorded in the presence of **AQ** (Figure S20). A broad CT band between **1** and **AQ** at around 410 nm gradually increased with increasing the amount of **AQ** from 1:1 to 1:5. The apparent color of the solution under ambient light changed to yellow.

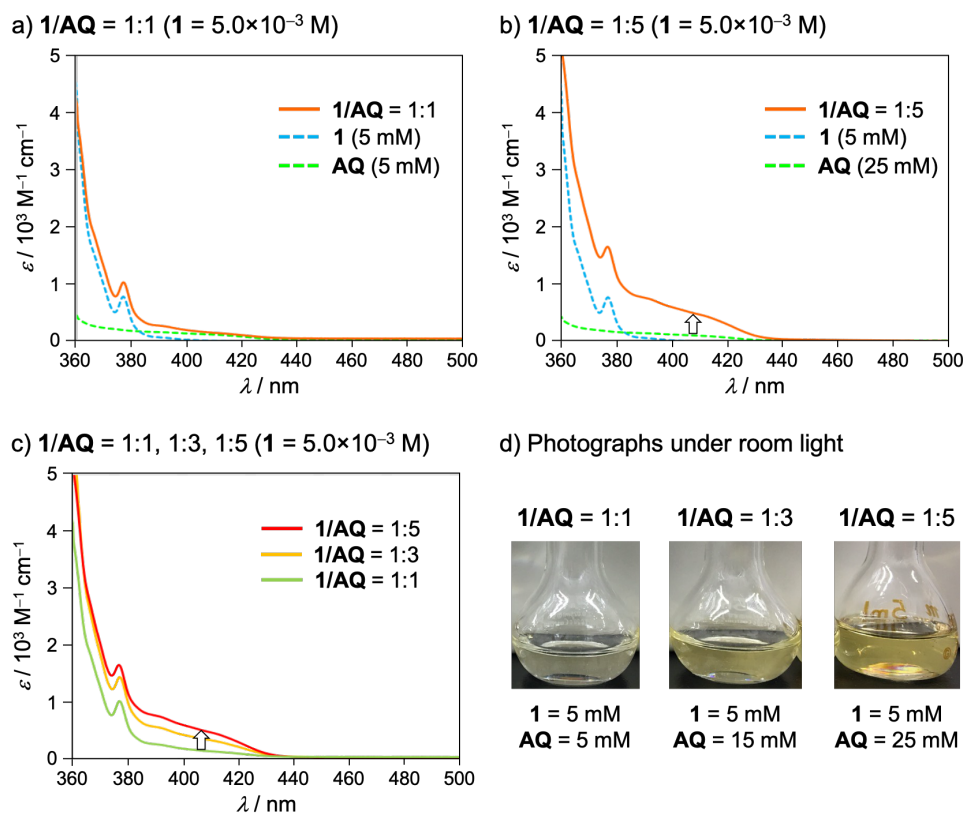
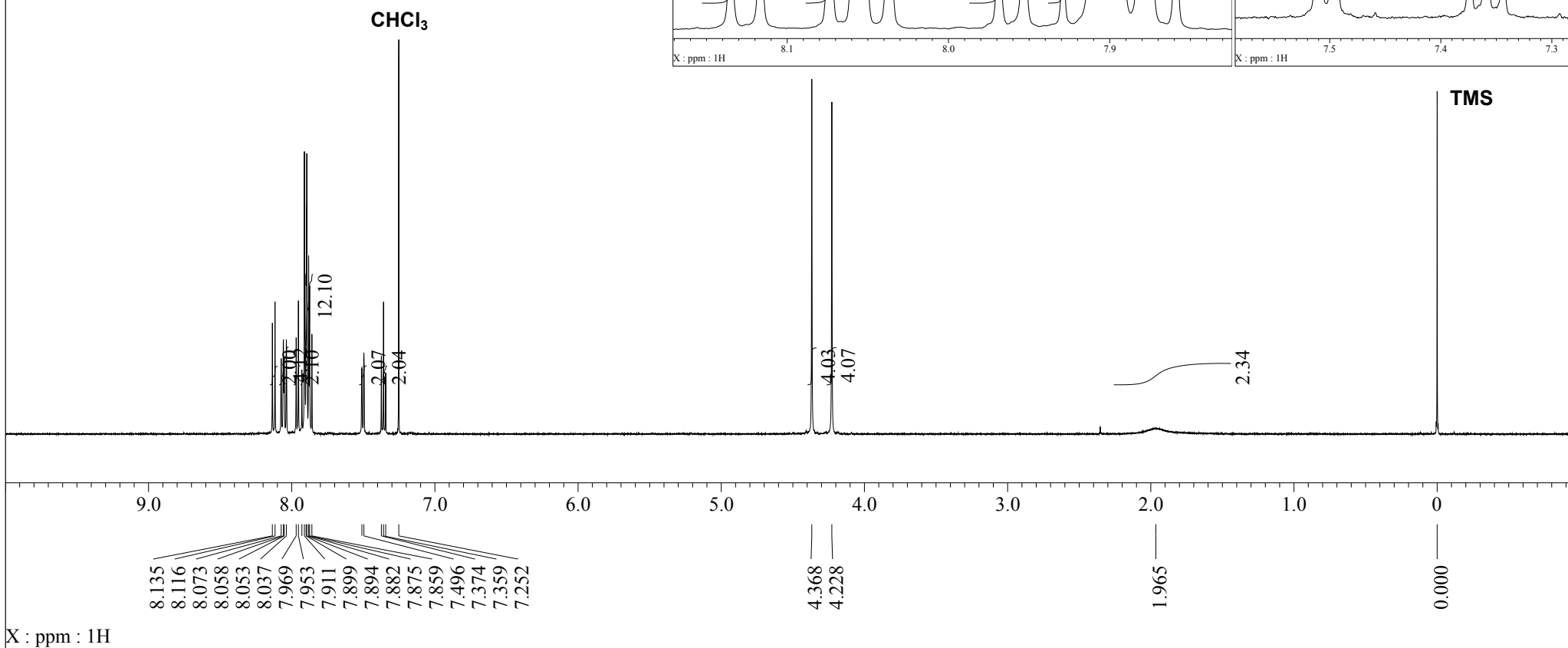
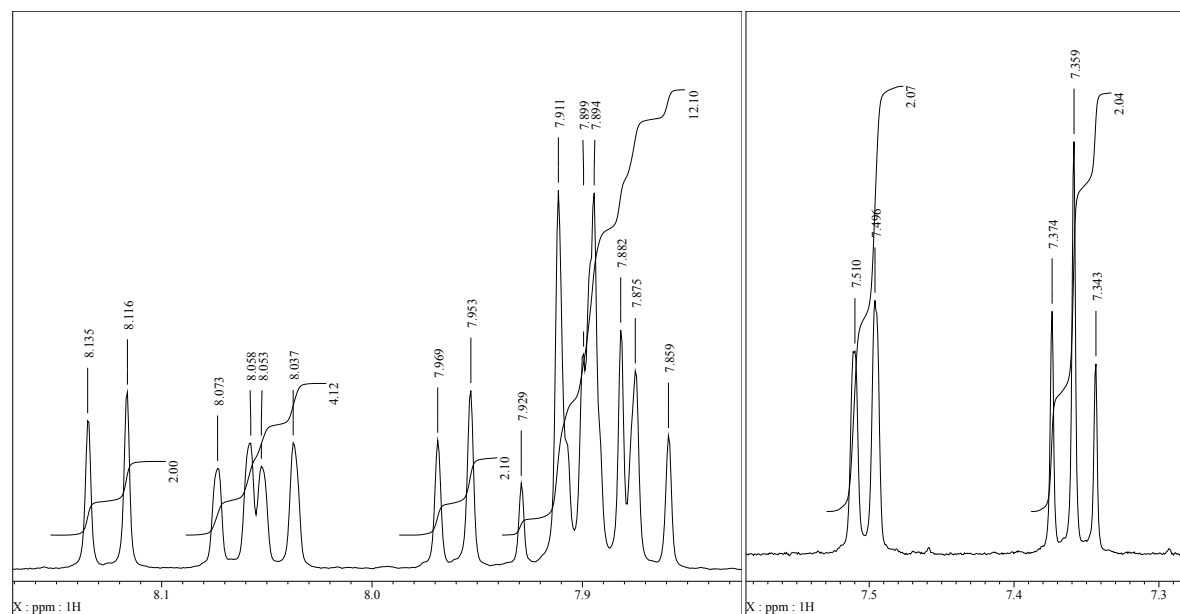
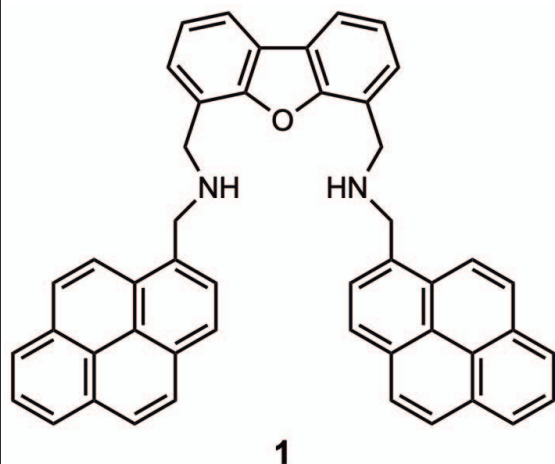
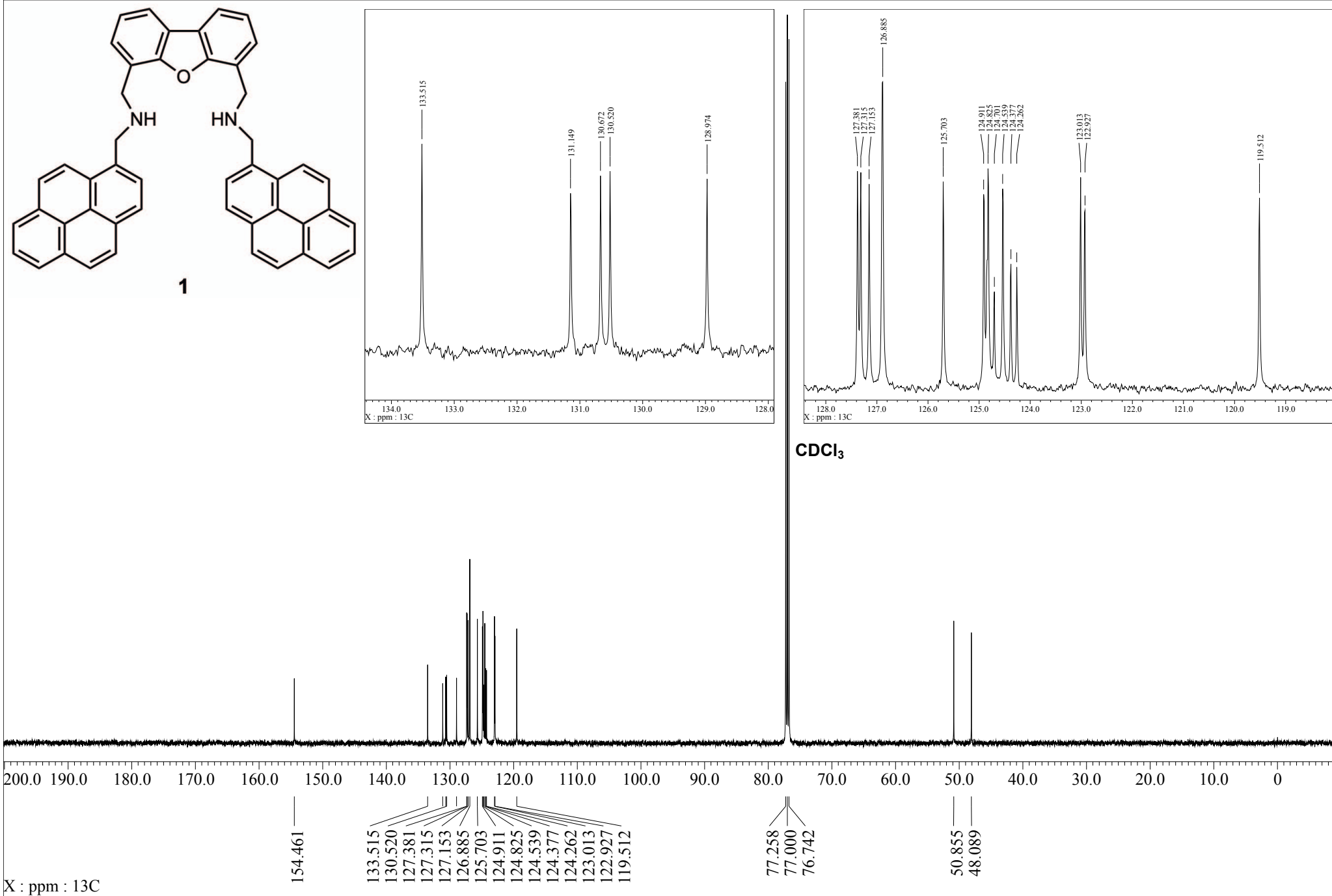


**Figure S20** a–c) Absorption spectra in chloroform. a)  $1/\text{AQ} = 1:1$  ( $1 = 5.0 \times 10^{-3} \text{ M}$ ), **1** (5 mM), and **AQ** (5 mM). b)  $1/\text{AQ} = 1:5$  ( $1 = 5.0 \times 10^{-3} \text{ M}$ ), **1** (5 mM), and **AQ** (25 mM). c)  $1/\text{AQ} = 1:1, 1:3,$  and  $1:5$  ( $1 = 5.0 \times 10^{-3} \text{ M}$ ). d) Photographs for  $1/\text{AQ}$  in chloroform solutions under room light.

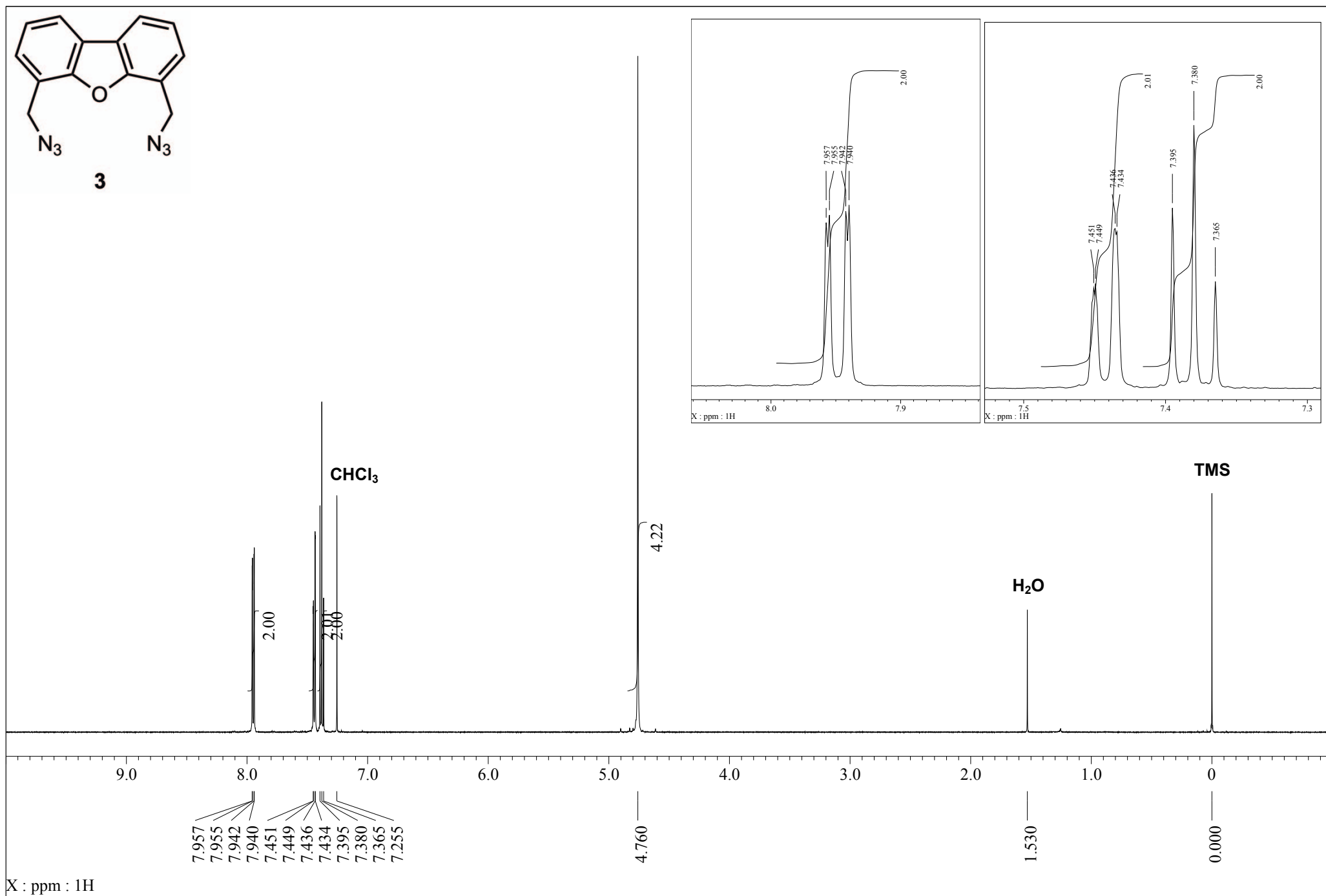
<sup>1</sup>H NMR spectrum of 1 (500 MHz, in CDCl<sub>3</sub>, rt)



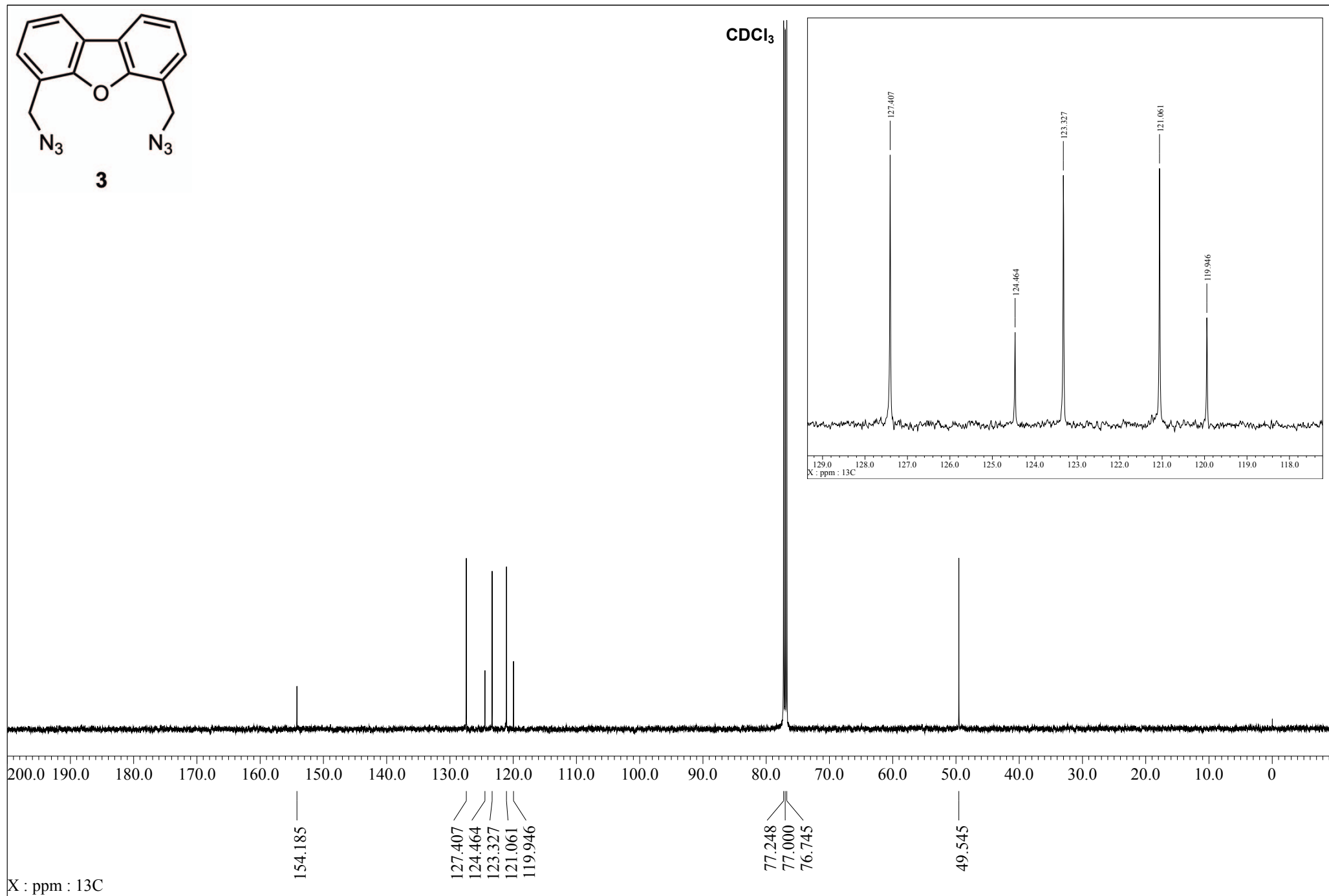
<sup>13</sup>C NMR spectrum of 1 (126 MHz, in CDCl<sub>3</sub>, rt)



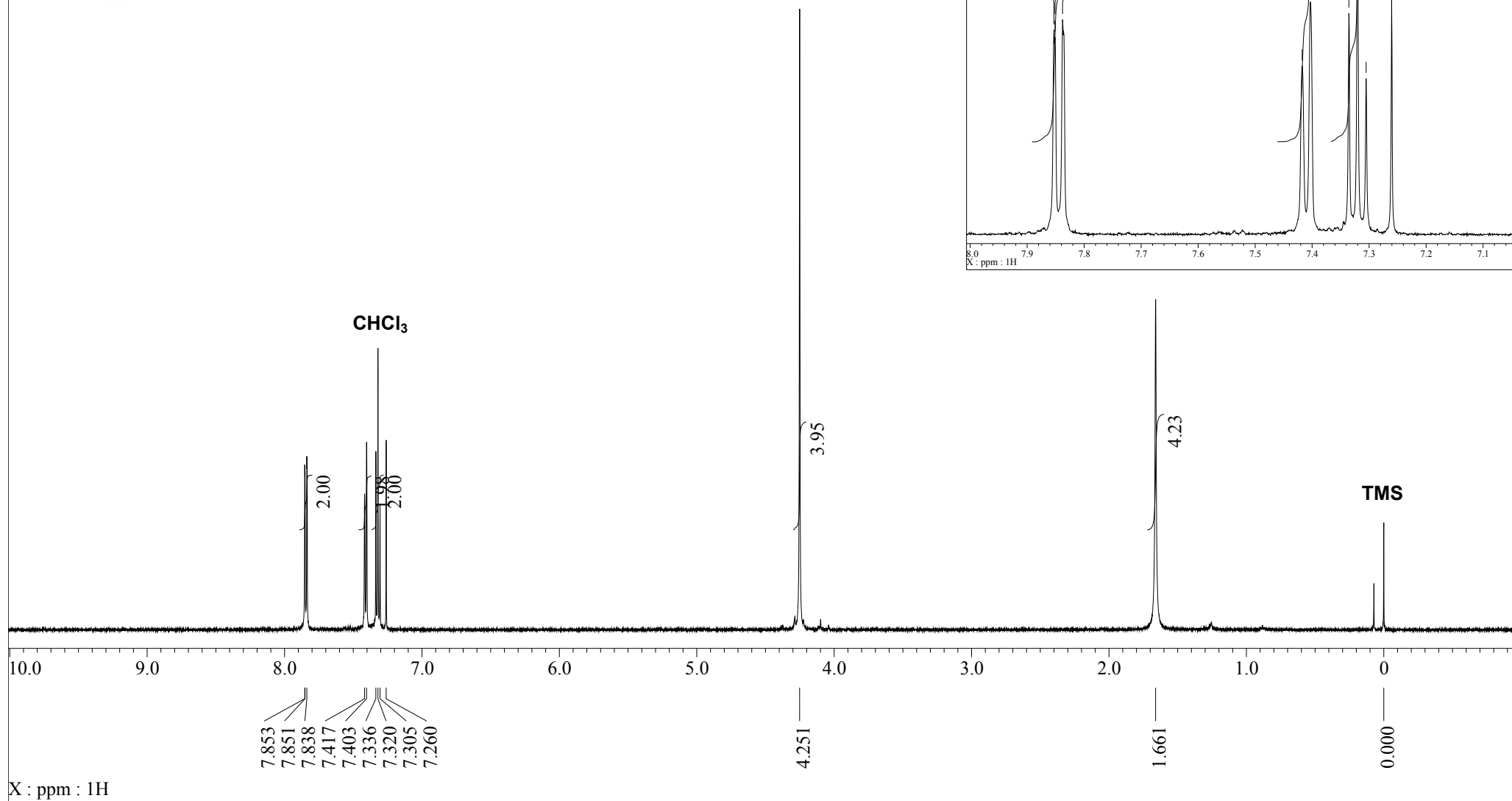
<sup>1</sup>H NMR spectrum of 3 (500 MHz, in CDCl<sub>3</sub>, rt)



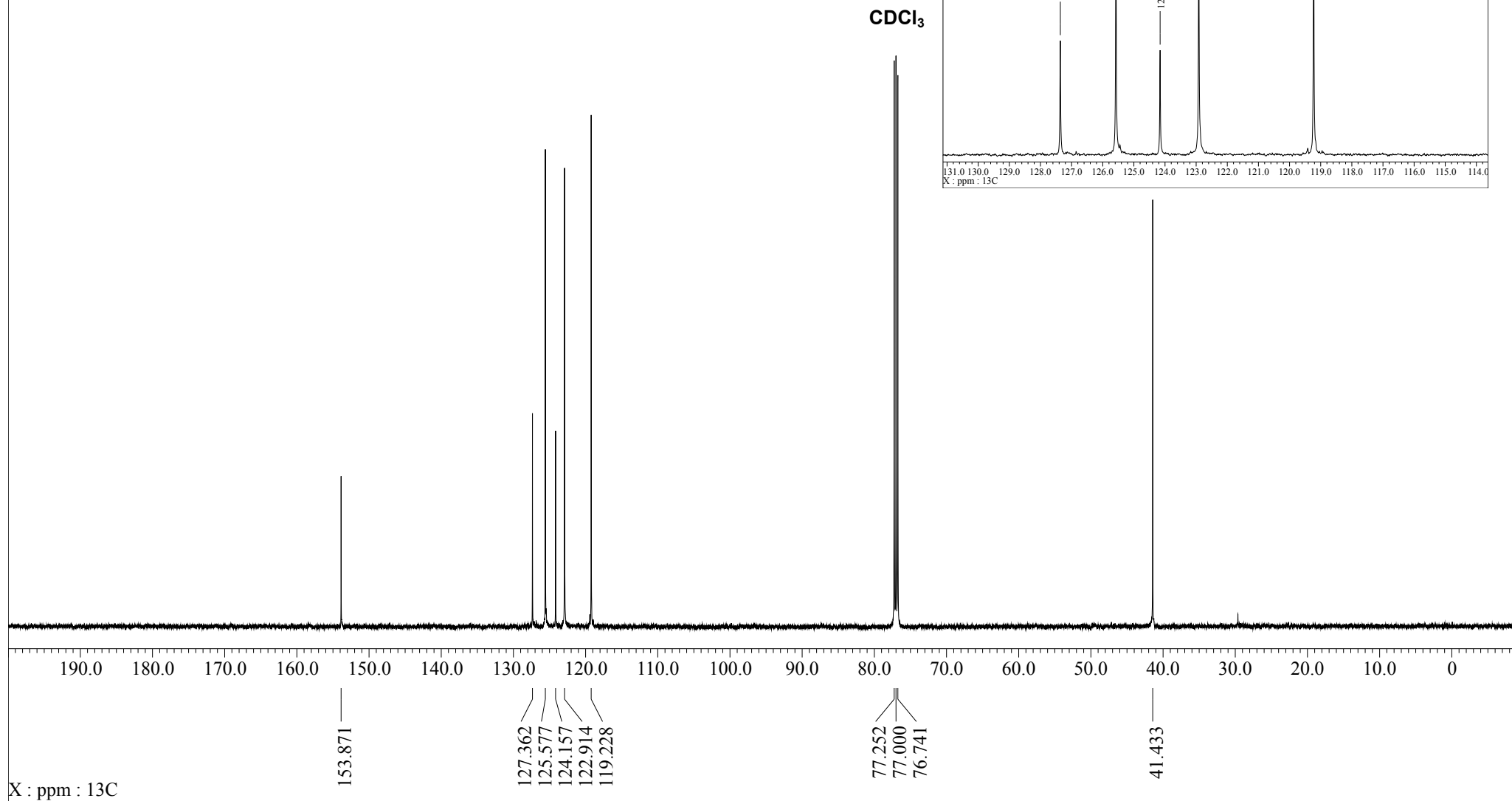
<sup>13</sup>C NMR spectrum of 3 (126 MHz, in CDCl<sub>3</sub>, rt)



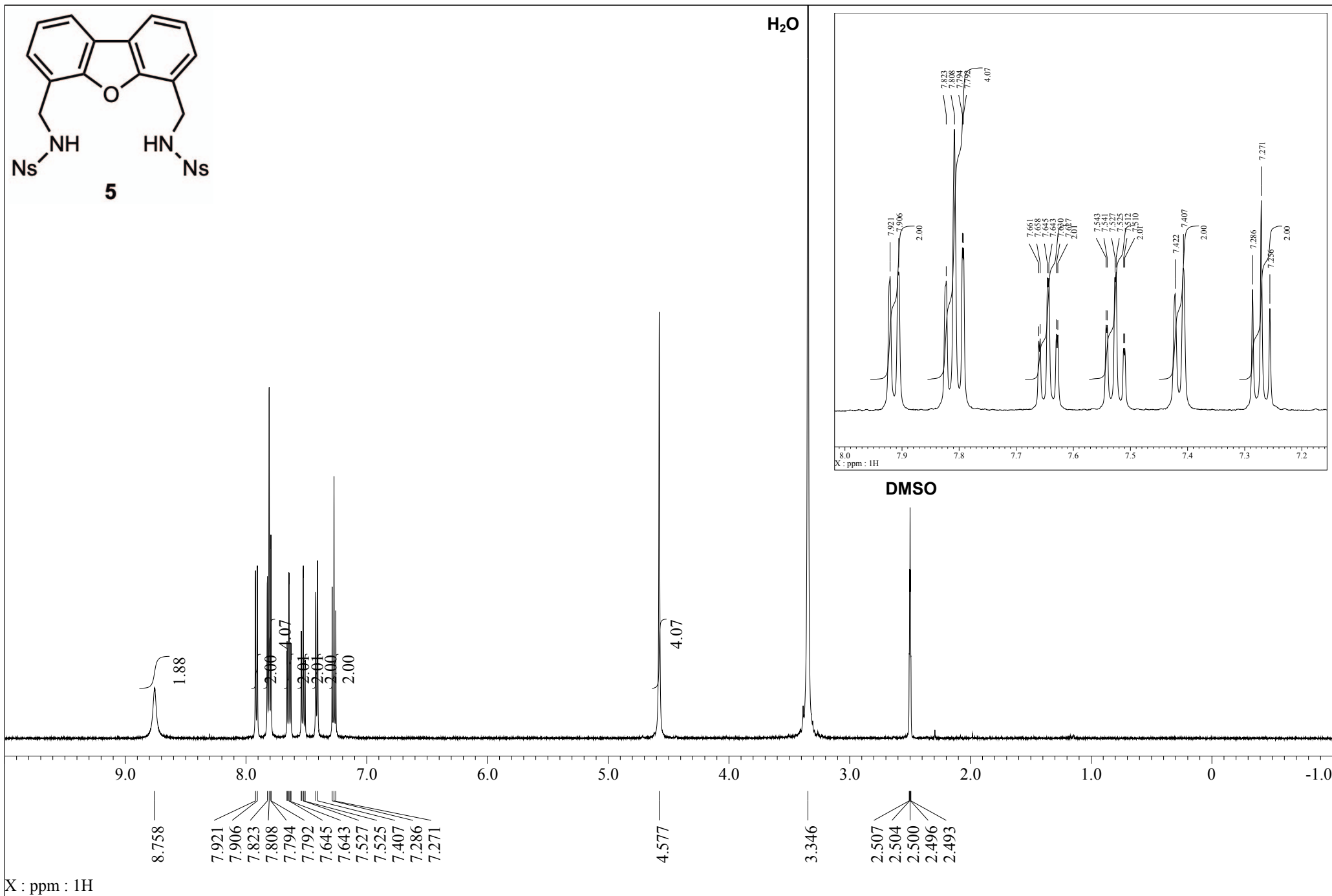
<sup>1</sup>H NMR spectrum of 4 (500 MHz, in CDCl<sub>3</sub>, rt)



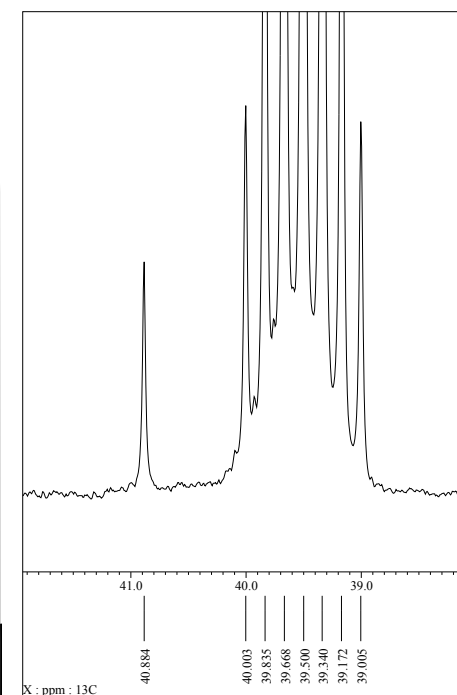
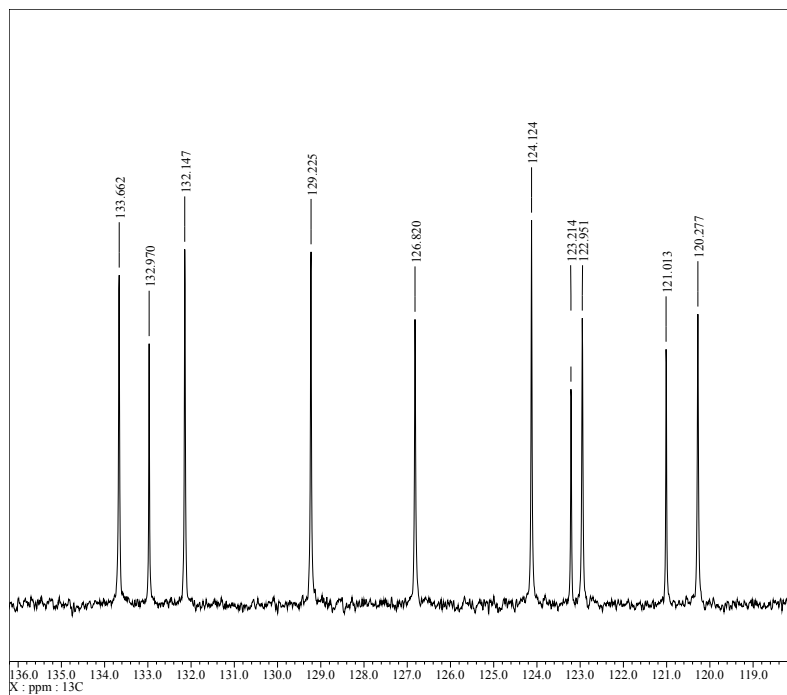
<sup>13</sup>C NMR spectrum of 4 (126 MHz, in CDCl<sub>3</sub>, rt)



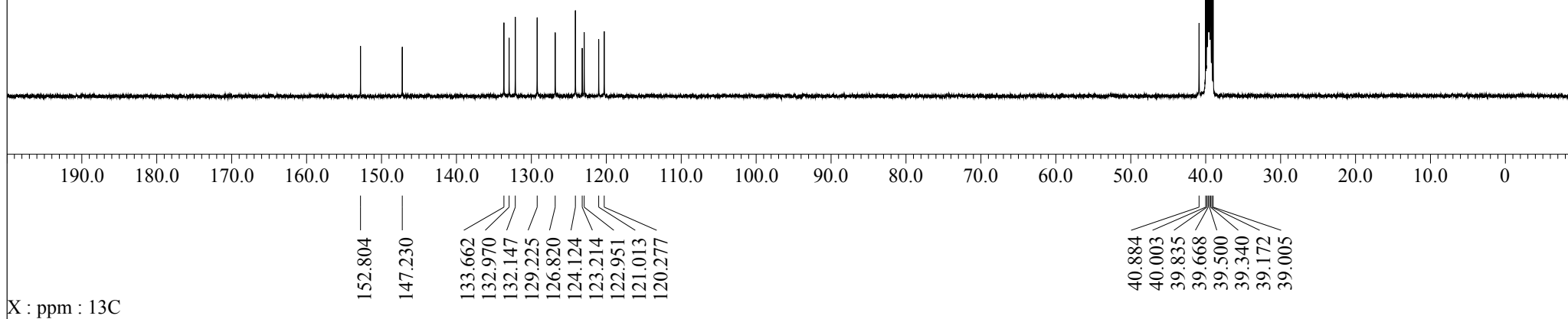
<sup>1</sup>H NMR spectrum of 5 (500 MHz, in DMSO-d<sub>6</sub>, rt)



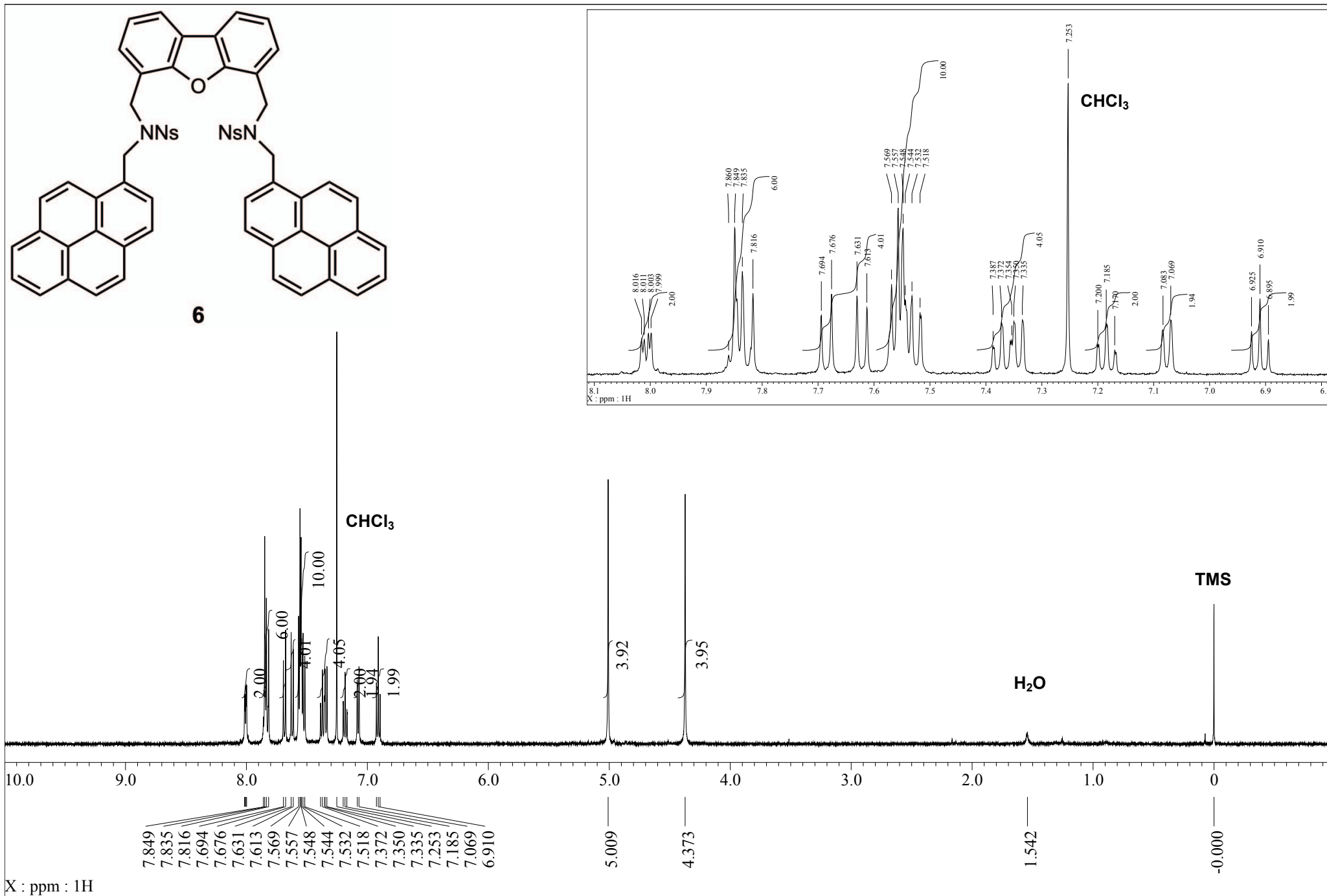
<sup>13</sup>C NMR spectrum of 5 (126 MHz, in DMSO-d<sub>6</sub>, rt)



DMSO-d<sub>6</sub>



<sup>1</sup>H NMR spectrum of 6 (500 MHz, in CDCl<sub>3</sub>, rt)



<sup>13</sup>C NMR spectrum of 6 (126 MHz, in CDCl<sub>3</sub>, rt)

